Available online at www.sciencedirect.com

ScienceDirect

Mendeleev Commun., 2017, **27**, 487–489

Mendeleev Communications

Microwave-assisted synthesis of magnetic iron oxide nanoparticles in oleylamine–oleic acid solutions

Tatiana A. Lastovina,* Andriy P. Budnyk, Mikhail A. Soldatov, Yury V. Rusalev, Alexander A. Guda, Alena S. Bogdan and Alexander V. Soldatov

International Research Center 'Smart Materials', Southern Federal University, 344090 Rostov-on-Don, Russian Federation. E-mail: lastovina@sfedu.ru

DOI: 10.1016/j.mencom.2017.09.019

Using microwave-assisted synthesis in organic solution, we produced magnetic γ-Fe_2O_3 nanoparticles covered with oleylamine and oleic acid.

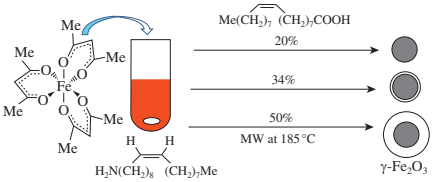

Magnetic nanoparticles (MNPs) are of interest because of their potential applications in biomedicine and electronics.[1] Magnetite (Fe_3O_4) and maghemite (γ-Fe_2O_3) MNPs are the most commonly used contrast agents in magnetic resonance imaging (MRI).[2] Their magnetic properties can be improved by doping with rare-earth elements (Eu^{3+}, Sm^{3+} and Gd^{3+}).[3] The best functionality of MNPs comes from a good match of the right size and shape for membrane penetration in a living body, evident magnetization for a response to external magnetic fields and the presence of a proper surface coating for biocompatibility with immune system.[1,2]

Synthetic approaches for the production of MNPs[4] include the use of chemical co-precipitation, microemulsions, thermal decomposition and the aerosol spray pyrolysis or oxidation of iron in aerated aqueous solutions.[5] In comparison with conventional heating techniques, microwave (MW) heating has additional advantages (higher heating rates and precise heating control), which provide the formation of highly crystalline uniform MNPs with monodisperse size distribution; it significantly shortens the synthesis time and requires less energy consumption.[6] Naked MNPs tend to aggregate due to magnetic dipole–dipole interactions. To prevent this, surfactants such as poly(ethylene glycol), chitosan, and dextran are used.[1]

A combination of oleic acid with oleylamine has been frequently chosen for the shape-controlled synthesis of colloidal inorganic nanocrystals.[7] Hyeon *et al.*[8(a)] produced monodisperse maghemite MNPs of 4–16 nm by the decomposition of $Fe(CO)_5$ in dioctyl ether at 100 °C in the presence of oleic acid. Sun *et al.*[8(b)] prepared Fe_3O_4 by heating iron(III) acetylacetonate [$Fe(acac)_3$] with oleylamine and oleic acid in 1,2-hexadecanediol. Perez De Berti and co-workers underlined that, among these two iron precursors, $Fe(acac)_3$ is inexpensive and less toxic, and it has low moisture sensitivity. They synthesized γ-Fe_2O_3 MNPs with average sizes of 3–17 nm by the thermal decomposition of $Fe(acac)_3$ at 265 °C in oleic acid, oleylamine and diphenyl ether.[8(c)]

Here, we describe the properties of iron oxide MNPs obtained by the thermal decomposition of $Fe(acac)_3$ under MW heating at 185 °C in pure oleylamine and in a mixture of oleylamine and oleic acid taken in different quantities.† The synthesized samples were marked based on the oleic acid content (%) of the mixture and characterized by various techniques.‡

The XRD patterns of the samples (Figure 1) exhibit reflexes at 2θ of about 30, 35, 37, 43, 53, 57, 62 and 74°, which can be indexed into a cubic spinel structure. The average crystallite sizes calculated from the Scherrer–Debye equation[9] are 3.5, 5.3, 4.9 and 4.0 nm for the MNPs0, MNPs20, MNPs34 and MNPs50 samples, respectively.

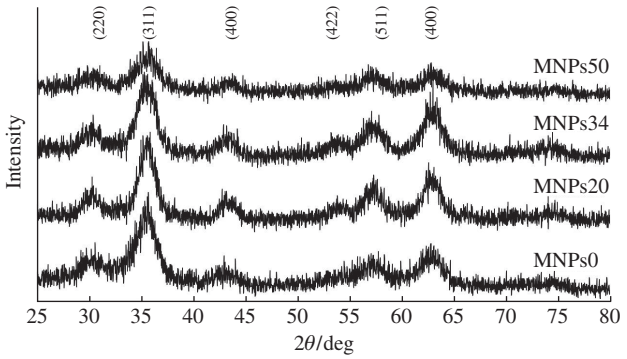

Figure 1 XRD patterns of MNPs samples.

† $Fe(acac)_3$ (0.2648 g) was dissolved in oleylamine or in a mixture of oleylamine and oleic acid. The following compositions were chosen: 18.8 ml oleylamine (MNPs0), 15 ml oleylamine + 3.8 ml oleic acid (MNPs20), 12.4 ml oleylamine + 6.4 ml oleic acid (MNPs34), and 9.4 ml oleylamine + 9.4 ml oleic acid (MNPs50). The mixture was placed in a Discover SP (CEM) MW oven and heated in two steps: at 120 °C for 1 h with stirring and at 185 °C for 1.5 h. After cooling, the precipitate was washed several times with absolute ethanol (keeping powder by a magnet) and dried at 60 °C in a vacuum oven.

‡ X-ray diffraction (XRD) patterns were recorded using a D2 Phaser (Bruker) diffractometer (CuKα radiation, λ = 0.15406 nm). Transmission electron microscopy (TEM) images were acquired on a G2 Spirit BioTWIN (Tecnai) microscope operated at an accelerating voltage of 120 kV. X-ray absorption spectra were measured by means of Looper R-XAS (Rigaku) laboratory X-ray absorption spectrometer in the transmission mode using a Ge311 monochromator. Magnetic susceptibility measurements were performed with a Vibrating Sample Magnetometer (VSM) 7400 (Lakeshore). The Fourier transform Infrared (FTIR) spectrum was measured on a Vertex 70 (Bruker) spectrometer with a resolution of 2 cm^{-1} on an Attenuated total reflectance (ATR) accessory. All measurements were performed at room temperature.

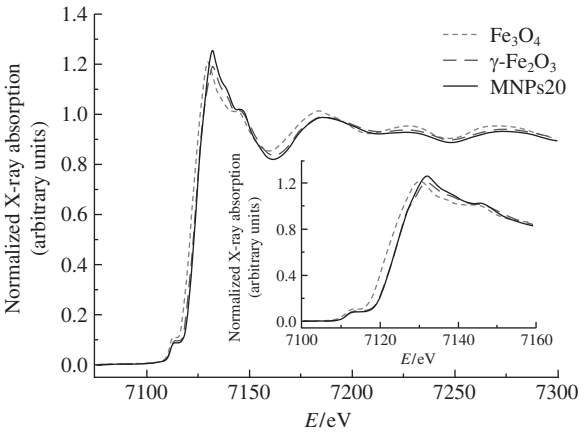

Figure 2 Fe K-edge XANES spectra of MNPs20 compared to Fe_3O_4 and γ-Fe_2O_3 iron oxide bulk references.

In order to distinguish between the two spinel phases of Fe_3O_4 and γ-Fe_2O_3, the Fe K-edge X-ray absorption near edge structure (XANES) spectra were measured for MNPs20 sample. Figure 2 shows the comparison of MNPs20 XANES to both Fe_3O_4 and γ-Fe_2O_3 bulk references. Local atomic and electronic structures of Fe_3O_4 and γ-Fe_2O_3 have two main distinctions. On the one hand, γ-Fe_2O_3 is purely Fe^{3+}, while Fe_3O_4 is a mixture of Fe^{2+} (33%) and Fe^{3+} (67%). On the other hand, the γ-Fe_2O_3 phase is significantly affected by defects, leading to a different Fe coordination. The chemical shift of the rising edge is evidently seen in the XANES spectra of Fe_3O_4 and γ-Fe_2O_3 reference compounds. The MNPs20 XANES spectrum shows the same chemical shift as that of γ-Fe_2O_3, implying pure Fe^{3+} configuration. X-ray absorption fine structure is extremely sensitive to interatomic distances and coordination numbers. Based on the experimental spectra features, positions and intensities at 7185, 7226 and 7275 eV, it could be suggested that MNPs20 has a local atomic coordination similar to that of a γ-Fe_2O_3 phase.

The TEM images (Figure 3) show that the addition of oleic acid to the reaction mixture reduces the extent of NP aggregation, as compared with pure oleylamine. The MNPs are covered by an organic shell.

The FTIR ATR spectra (Figure 4) provide essential details of the surface coverage of MNPs. The spectra contain Fe–O vibration modes in the envelope below 700 cm^{-1} (MNPs0 sample). In the mid-IR region, both MNPs0 and MNPs20 exhibit organic traces, while the remaining couple of samples provide an intense spectral fingerprint. This profile contains bands from the functional groups of both oleic acid and oleylamine molecules: $\nu_{as}/\nu_s(CH_2)$ at 2913/2848 cm^{-1} with respective $\delta(CH_2)$ at 1469 and 718 cm^{-1}, $\nu(NH_2)$ at 3310 cm^{-1} and $\delta(NH_2)$ at 1534 cm^{-1}, ν(C=C) at 1632 cm^{-1}, *etc*. The red shift of the bands and the absence of ν(C=O) at 1710 cm^{-1} suggest that oleic acid is bonded to MNPs *via* the COO^- group (1560 and 1417 cm^{-1}).[7,10] The exact arrangement of these surfactants on the surface of MNPs is still under study taking into account some models proposed in the literature.[11]

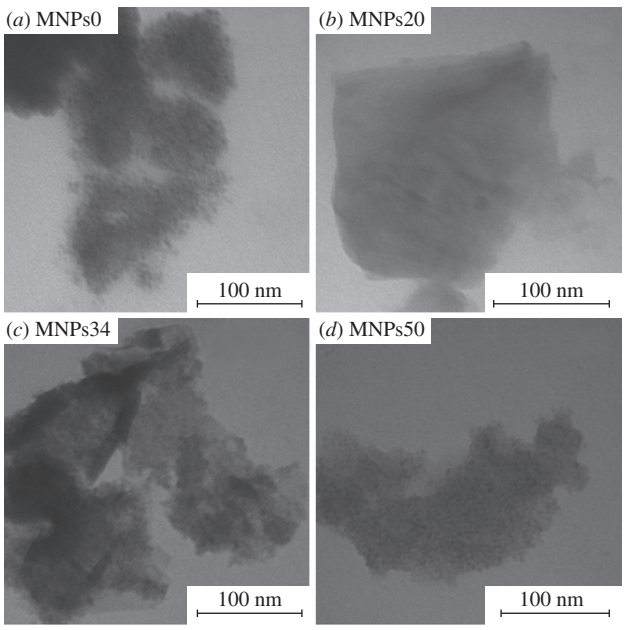

Figure 3 TEM images for MNPs samples.

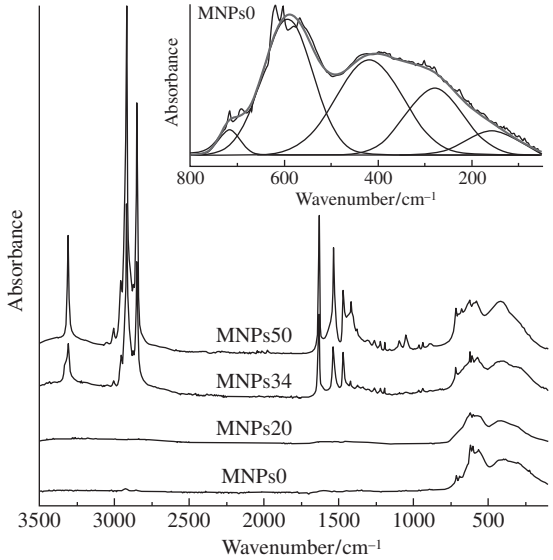

Figure 4 FTIR ATR spectra of MNPs samples. Inset: fitting Gaussians for the low-frequency spectral envelope of MNPs0 sample.

Figure 5 illustrates the magnetic properties of MNPs samples. The curves have similar profiles but different magnetization values. There is a clear trend from supermagnetic to paramagnetic properties with increasing the amount of oleic acid. Only the sample MNPs20 (MNPs prepared in a solution with 20 vol% oleic acid) has sufficiently large particles to exhibit a hysteresis (inset in Figure 5).

In conclusion, we have performed the thermal decomposition of an iron precursor in a binary mixture of oleic acid and oleylamine to produce γ-Fe_2O_3 MNPs of about 5 nm at all ratios between oleic acid and oleylamine. With the use of microwave heating, we have obtained the single-phase crystalline MNPs with clean surfaces or covered by surfactants. The addition of oleic acid to the reaction mixture reduces the extent of NP aggregation. The MNPs prepared in an oleylamine/oleic acid solution

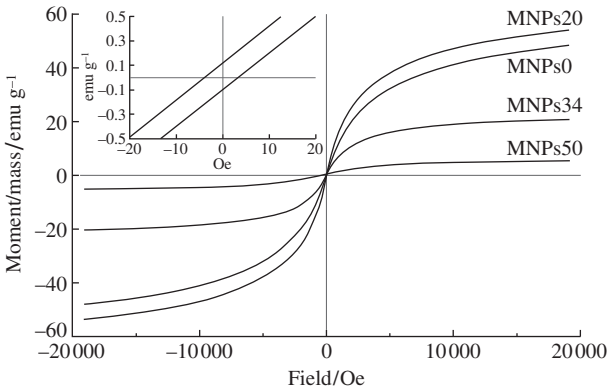

Figure 5 Magnetic moment *vs.* applied magnetic field curves for MNPs samples. The inset shows a zoom of MNPs20.

with 20 vol% oleic acid possess higher magnetic properties. These MNPs are promising candidates to be employed as MRI agents.[1]

This study was supported by the Russian Science Foundation (project no. 14-35-00051).

References

1 (*a*) S. Mornet, S. Vasseur, F. Grasset and E. Duguet, *J. Mater. Chem.*, 2014, **14**, 2161; (*b*) S. Singamaneni, V. N. Bliznyuk, C. Binek and E. Y. Tsymbal, *J. Mater. Chem.*, 2011, **21**, 16819; (*c*) A. Yu. Soloveva, Yu. V. Ioni and S. P. Gubin, *Mendeleev Commun*., 2016, **26**, 38.

2 M. Di Marco, C. Sadun, M. Port, I. Guilbert, P. Couvreur and C. Dubernet, *Int. J. Nanomedicine*, 2007, **2**, 609.

3 T. A. Lastovina, A. L. Bugaev, S. P. Kubrin, E. A. Kudryavtsev and A. V. Soldatov, *J. Struct. Chem.*, 2016, **57**, 1444 (*Zh. Strukt. Khim.*, 2016, **57**, 1523).

4 (*a*) E. Tombácz, R. Turcu, V. Socoliuc and L. Vékás, *Biochem. Biophys. Res. Commun*., 2015, **468**, 442; (*b*) I. N. Topchieva, V. V. Spiridonov, A. N. Zakharov, M. I. Afanasov, A.V. Mironov, N. S. Perov and A. S. Semisalova, *Mendeleev Commun.*, 2015, **25**, 145.

5 (*a*) A. E. Chekanova, A. L. Dubov, E. A. Goodilin, E. A. Eremina, A. Birkner, Yu. V. Maximov, I. P. Suzdalev, V. N. Uvarov, A. D. Shevchenko and Yu. D. Tretyakov, *Mendeleev Commun.*, 2009, **19**, 4; (*b*) A. Yu. Vasil'kov, D. A. Migulin, A. V. Naumkin, O. A. Belyakova, Ya. V. Zubavichus, S. S. Abramchuk, Yu. V. Maksimov, S. V. Novichikhin and A. M. Muzafarov, *Mendeleev Commun.*, 2016, **26**, 187.

6 (*a*) W. Xiao, H. Gu, D. Li, D. Chen, X. Deng, Z. Jiao and J. Lin, *J. Magn. Magn. Mater.*, 2012, **324**, 488; (*b*) D. A. Jones, T. P. Lelyveld, S. D. Mavrofidis, S. W. Kingman and N. J. Miles, *Resour. Conserv. Recycl.*, 2002, **34**, 75.

7 W. Bu, Z. Chen, F. Chen and J. Shi, *J. Phys. Chem. C*, 2009, **113**, 12176.

8 (*a*) T. Hyeon, S. S. Lee, J. Park, Y. Chung and H. B. Na, *J. Am. Chem. Soc*., 2001, **123**, 12798; (*b*) S. Sun, H. Zeng, D. B. Robinson, S. Raoux, P. M. Rice, S. X. Wang and G. Li, *J. Am. Chem. Soc.*, 2004, **126**, 273; (*c*) I. O. Perez De Berti, M. V. Cagnoli, G. Pecchi, J. L. Alessandrini, S. J. Stewart, J. F. Bengoa and S. G. Marchetti, *Nanotechnology*, 2013, **24**, 175601.

9 H. P. Klug and L. E. Alexander, *X-ray Diffraction Procedures for Polycrystalline and Amorphous Materials*, John Wiley & Sons, New York, 1962, pp. 491–538.

10 L. Zhang, R. He and H.-C. Gu, *Appl. Surf. Sci*., 2006, **253**, 2611.

11 (*a*) R. A. Harris, P. M. Shumbula and H. van der Walt, *Langmuir*, 2015, **31**, 3934; (*b*) M. Devaraj, R. Saravanan, R. K. Deivasigamani, V. K. Gupta, F. Gracia and S. Jayadevan, *J. Mol. Liq.*, 2016, **221**, 930; (*c*) K. Yang, H. Peng, Y. Wen and N. Li, *Appl. Surf. Sci*., 2010, **256**, 3093.

Received: 12th December 2016; Com. 16/5118